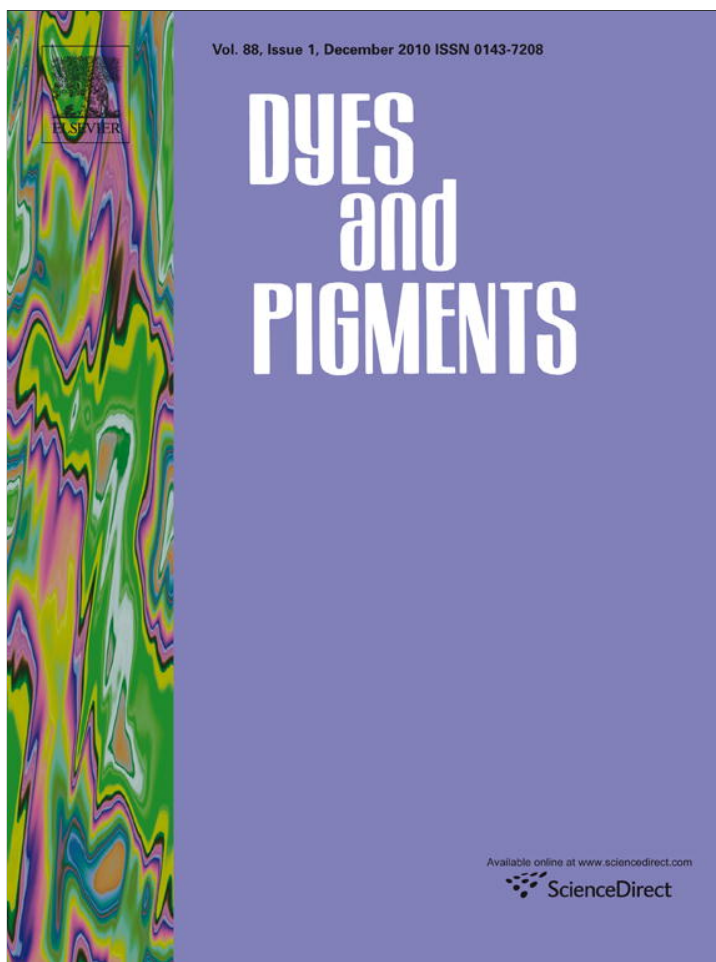


Provided for non-commercial research and education use.
Not for reproduction, distribution or commercial use.



(This is a sample cover image for this issue. The actual cover is not yet available at this time.)

This article appeared in a journal published by Elsevier. The attached copy is furnished to the author for internal non-commercial research and education use, including for instruction at the authors institution and sharing with colleagues.

Other uses, including reproduction and distribution, or selling or licensing copies, or posting to personal, institutional or third party websites are prohibited.

In most cases authors are permitted to post their version of the article (e.g. in Word or Tex form) to their personal website or institutional repository. Authors requiring further information regarding Elsevier's archiving and manuscript policies are encouraged to visit:

<http://www.elsevier.com/copyright>



Metal enhanced fluorescence of the fluorescent brightening agent Tinopal-CBX near silver island film

Hirdyesh Mishra^a, Yongxia Zhang^a, Chris D. Geddes^{a,b,*}

^a Institute of Fluorescence, University of Maryland Baltimore County, 701 East Pratt Street, Baltimore, MD 21202, USA

^b Department of Chemistry, University of Maryland Baltimore County, 701 East Pratt Street, Baltimore, MD 21202, USA

ARTICLE INFO

Article history:

Received 14 July 2010

Received in revised form

21 February 2011

Accepted 4 March 2011

Available online 17 March 2011

Keywords:

Metal-enhanced fluorescence

Optical brightener tinopal-CBS

Surface plasmons

Plasmon enhanced fluorescence

Surface plasmon enhanced fluorescence

Photostability

ABSTRACT

Metal-enhanced fluorescence (MEF) studies of the optical brightener Tinopal-CBS (4,4'-distyrylbiphenyl sulfonic sodium salt) have been undertaken using steady-state and time resolved fluorescence measurements on silver island films (SiFs) deposited on glass slides and silver nano-particles adsorbed onto cellulose based filter paper. Nearly a 4.5 fold enhancement in fluorescence intensity is observed from both SiFs and nano-particle deposited cellulose filter paper. In addition an enhanced photostability and decrease in decay time is also observed on SiFs. These results are consistent with two distinct mechanisms of MEF, firstly coupling and transferring of the excited states energies of fluorophores to surface plasmons in the silver island deposited glass films, and secondly, an electric field enhancement effect, which facilitates enhanced absorption of the fluorophores. Our findings reveal significant benefits of enhanced luminescence and prolonged photostability of Tinopal CBS. As such, Plasmon-tinopal constructs offer new material opportunities as well as multifarious applications in the life sciences.

© 2011 Elsevier Ltd. All rights reserved.

1. Introduction

Recently in the advancement of near-field spectroscopy, the metal-enhanced fluorescence (MEF) technology [1–3] has become a powerful tool to investigate the structure and dynamics of molecules near-to metallic nano-particles i.e. in the near field. Due to surface plasmons interactions, the photo-physical properties of molecules are found to be both drastically and favorably changed in ways which enhance emission and improve fluorophores photostability.

Over the last several years Geddes and coworkers [4–7] have developed a mechanistic interpolate as well as numerous applications of MEF from various metallic surfaces. In MEF, in addition to the enhancement in fluorescence, decreases in decay times and increases in photo stabilities along with angular-dependent emission are also frequently observed. Our current interpretation of MEF has been underpinned by a model whereby non-radiative energy transfer occurs from excited fluorophores to surface plasmons in non-continuous films, Scheme 1.

Tinopal-CBS is a fluorescent whitening agent and widely used to improve the appearance of various commercial products viz.

washing powder, plastics, paper, paints, textile etc. [8–12] In addition, tinopal is also used in the clinical biosciences to detect human fecal contamination in water [13], rapid recognition of pulmonary dirofilariasis [14], Peroral infection of nuclear polyhedrosis virus [15] in bio-pesticides to understand the growth of crops [16], studying the behavior of pollinators [17–19] in soil spray analysis [20] and cellulose fiber analysis [21], to name but just a few examples. Tinopal-CBS is a sulfonic sodium salt of 4,4'-distyrylbiphenyl which readily absorbs UV radiation and emits a strong blue fluorescence in the wavelength range from 400 to 550 nm [13]. In the present paper, we report the dramatic change observed in the photophysics of Tinopal-CBS on silver islands deposited on both glass slides and also adsorbed onto silver nanoparticles deposited cellulose filter paper demonstrating significant further utility of tinopal-CBS. About ≈ 4.5 fold enhancement in far-field tinopal fluorescence is observed with near-field enhancement values about 50 fold greater, i.e. 225-fold as compared to a control sample containing no silver.

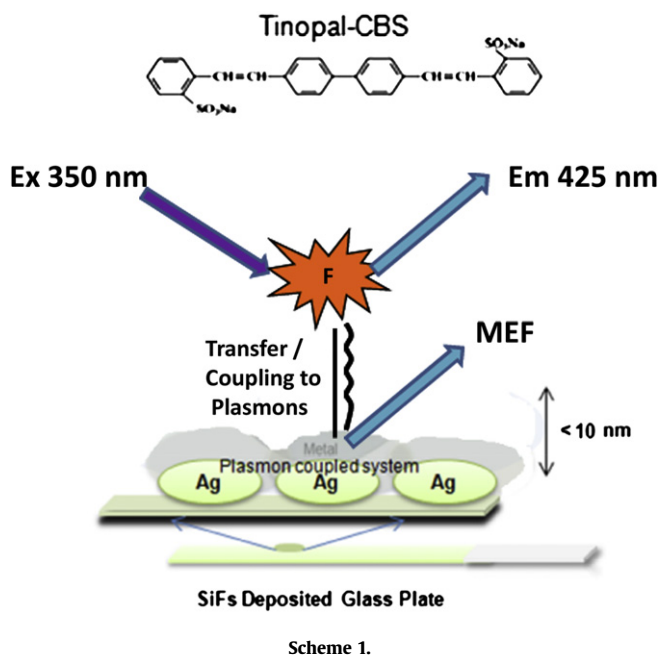
2. Experimental section

2.1. Materials

Tinopal-CBS was purchased from Tokyo Kasei Kogyo .Co. Ltd, Japan. Silane-prep glass microscope slides, Silver nitrate (99.9%),

* Corresponding author. Institute of Fluorescence, University of Maryland Baltimore County, 701 East Pratt Street, Baltimore, MD 21202, USA. Tel.: +1 410 576 5720; fax: +1 410 576 5722.

E-mail address: geddes@umbc.edu (C.D. Geddes).



sodium hydroxide (99.996%), ammoniumhydroxide (90%), D-glucose, ethanol (HPLC/ spectrophotometric grade), were purchased from Sigma–Aldrich Chemical company (Milwaukee, WI, USA). Quartz (75 mm × 25 mm) slides were purchased from Ted Pella Inc. CA, USA. The synthesis of silver colloids and SiFs were prepared according to previously published procedures [2]. The synthesis of silver colloids was undertaken using the following procedure: 2 ml of 1.16 mM trisodium citrate solution was added drop wise to a heated (90 °C) 98 ml aqueous solution of 0.65 mM silver nitrate while stirring. The mixture was heated for 10 min, and then cooled in ice until use. This procedure yields ca. 50 nm silver colloids as confirmed by TEM analysis. Three hundred micro-liters of tinopal dissolved in water was sandwiched between both the quartz slides and the SiFs coated quartz slides, respectively. Tinopal in water solution was subsequently pipetted onto the Ag colloid dried paper for the paper studies also.

Instrumentation Absorption spectra of tinopal on blank glass substrates and SiFs films were collected using a single beam Varian Cary 50–Bio UV–vis spectrophotometer. Emission spectra were collected using a Varian Cary Eclipse fluorescence spectrophotometer having a pulsed xenon source for excitation. A front face sample geometry was used to undertake all the fluorescence measurements with a slit width of 5 nm, both in the excitation monochromator and emission monochromator channels. Fluorescence decays were measured using a Horiba Jobin Yvon Tem-Pro fluorescence lifetime system employing the time-correlated single photon counting (TCSPC) technique, with a TBX picosecond detection module. The excitation source was a pulsed LED source of wavelength 372 nm having maximum repetition rate 1.0 MHz and pulse duration 1.1 nanosecond (FWHM). The intensity decays were analyzed by decay analysis software (DAS) version 6.4 in terms of the multi-exponential model: $I(t) = \sum_i \alpha_i \exp(-t/\tau_i)$ where α_i are the amplitudes and τ_i are the decay times, $\sum_i \alpha_i = 1.0$. The fractional contribution of each component to the steady state intensity is given by The values of α_i and τ_i were determined by nonlinear least squares impulse deconvolution analysis with the goodness of fit judged by the residual, autocorrelation function and χ^2 values. The measurement error in decay time analysis was of the order of 0.01 ns. Photo-stability experiments were undertaken using a 405 nm laser coupled with a neutral density filter and Ocean optics spectrophotometer HP2000. Real-color photographs of the fluorescence emission were taken through an emission filter with a Canon Power shot S50 Digital Camera. AFM images were performed on a Molecular Imaging Picoplus Microscope. Samples were imaged at a scan rate of 1 Hz with 512 × 512 pixel resolution in contact mode.

3. Results and discussions

SiFs are sub-wavelength size silver particles formed by reduction of silver nitrate on a glass surface. The absorption spectra of silver islands (SiFs) deposited for different times on glass slides are shown in Fig. 1(a). A broad structured absorption spectra ranging from 300 to 800 nm, having an absorption maximum at ≈ 380 nm is observed. On increasing the SiFs deposition time, the optical density of these films typically increases as shown in the inset of Fig. 1(a), along with slight change in structure. This indicates an increase in SiFs density on the glass slides. The decrease in

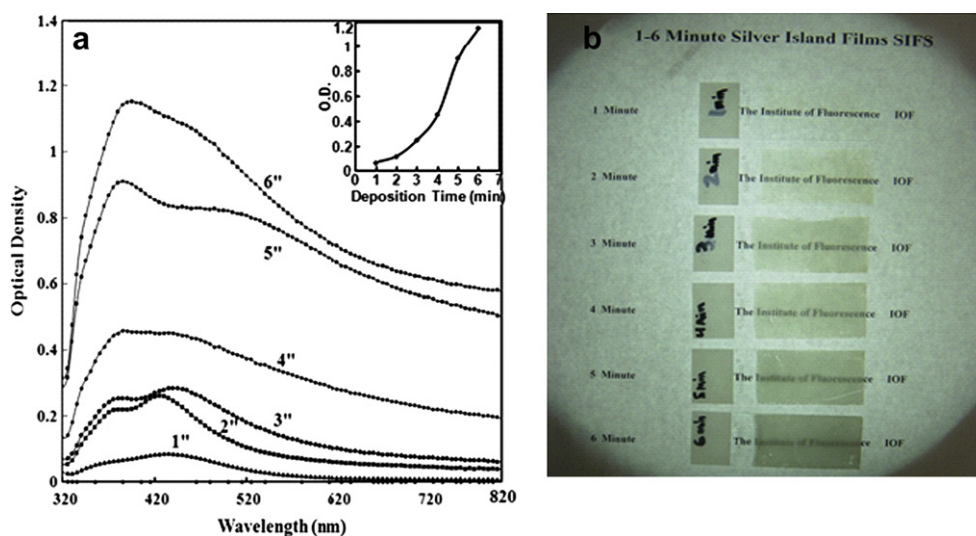


Fig. 1. (a) Absorption spectra and (b) Photograph of SiFs deposited on glass slides for different silver deposition times in minutes.

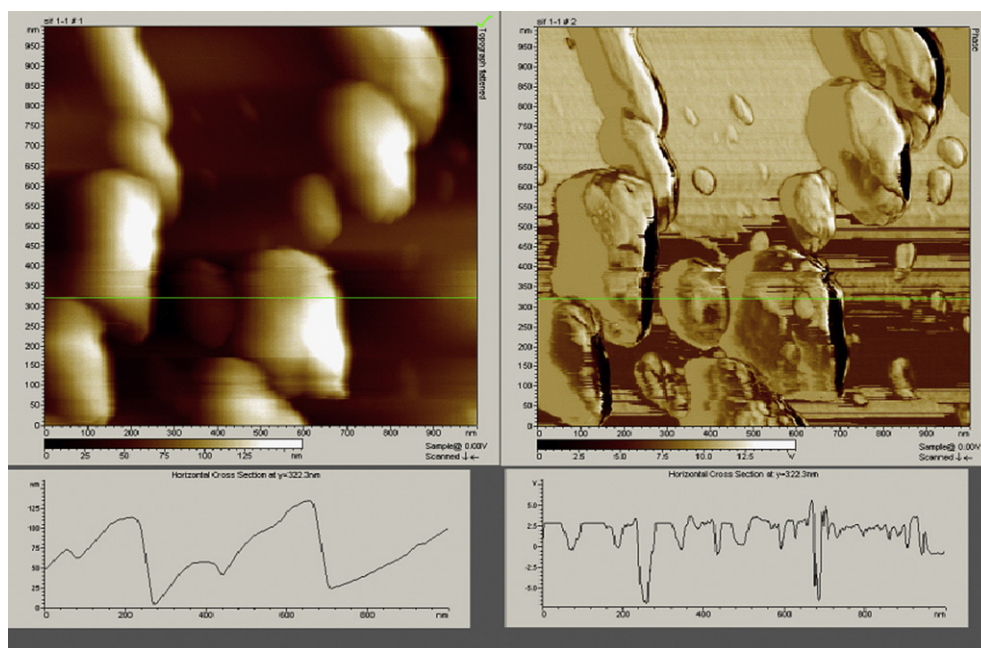


Fig. 2. AFM images of a SiFs film deposited on a glass slide: morphology image (Left) and Phase contrast image (Right) (Below are the respective line scans for the AFM images).

transparency is also shown in the real color photographs Fig. 1(b). AFM images of 4 min SiFs film deposited on glass slides are shown in Fig. 2. In this figure the morphology image of the SiFs is shown on the left and phase contrast image on the right. The surface morphology of metal nanostructured films provides for different properties in metal-enhanced fluorescence [6]. It can be seen that separated islands were formed on the glass slides, which is important for MEF i.e localized confined plasmons resonances.

Tinopal solution in water (concentration $\sim 10 \mu\text{M}$) shows a structured fluorescence spectra (maximum at 430 nm) along with an enhancement in fluorescence intensity from SiFs deposited glass slides Fig. 3(a) ($\lambda_{\text{ex}} = 350 \text{ nm}$). Nearly a 4.5 fold fluorescence enhancement observed for the 4 min deposited SiFs as shown in

the fluorescence enhancement factor verses deposition time graph, inset of Fig. 3(a). The enhancement factor is defined as the ratio of intensity observed from SiFs divided by that from a glass control substrate under otherwise identical conditions. The real color photographs show the enhanced luminescence. To understand the effect of silver islands on fluorescence structure, the spectrum of tinopal on glass and 4'' SiFs were normalized as shown in Fig. 3(b). It appears that the full width half maximum (FWHM) of the tinopal fluorescence spectra slightly decreases on SiFs, although for the most part is constant.

To understand further the slight changes in the FWHM and enhancement in fluorescence, absorption spectra of tinopal where measured in two different conditions as shown in Fig. 4. The

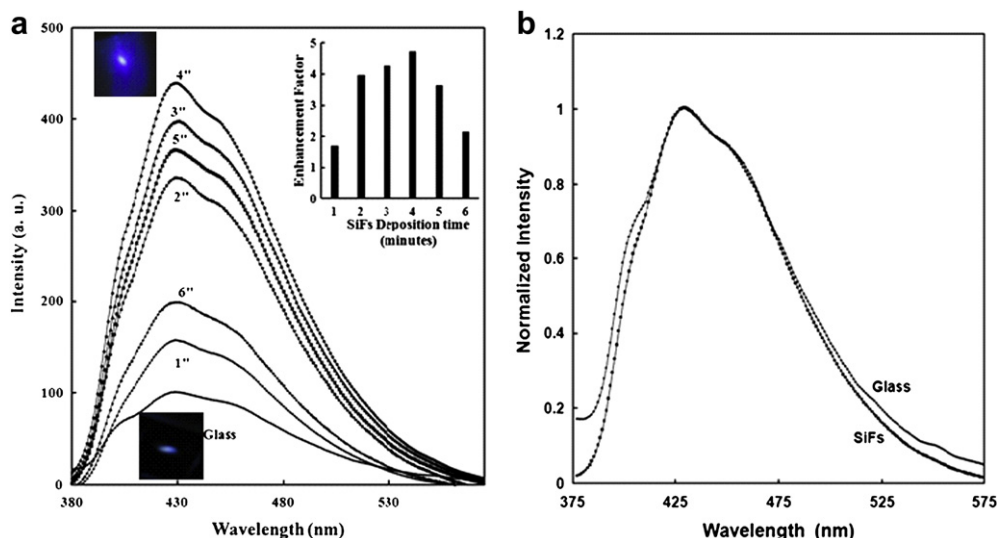


Fig. 3. (a) Emission spectrum of Tinopal on different SiFs and a glass slide (control sample). Enhancement factor is defined as the ratio of intensity observed from SiFs divided by that observed from a glass control substrate under otherwise identical conditions. (b) Normalized Fluorescence spectra of Tinopal on a glass slide and on SiFs (4''), wavelength of excitation $\lambda_{\text{ex}} = 350 \text{ nm}$ [Concentration 10^{-5} M].

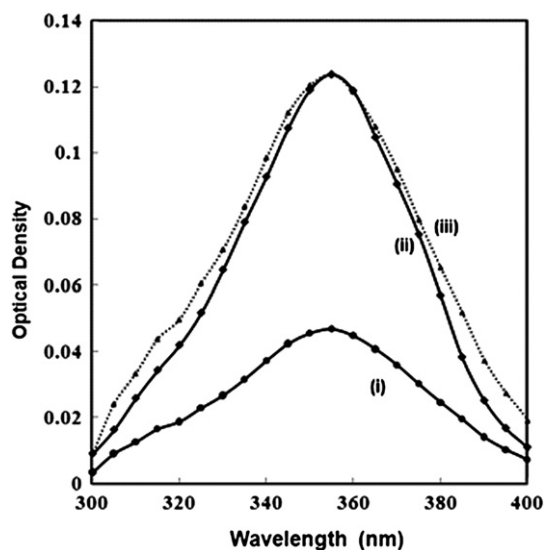


Fig. 4. Absorption spectra of tinopal (i) on a glass slide and (ii) on SiFs, (iii) normalized absorption spectra.

normalized spectrum Fig. 4 (iii) and show the decrease in FWHM of the absorption band in the presence of SiFs. Tinopal shows an absorption maximum on glass and SiFs at 349 nm, which is similar to the values reported in solution [9]. Nearly a 3.0 fold enhancement is observed in the absorbance of tinopal at 349 nm due to enhanced near field effect of SiFs by interaction with incident photon flux. The emission spectra is nearly 6345 cm⁻¹ Stoke shifted from the absorption band [9].

To understand the dynamics of the tinopal on SiFs surface, time resolved measurements of tinopal were undertaken on both glass and SiFs using time correlated single photon counting measurements. The analyzed decay data are given in Table 1. The respective analyzed overlapped time resolved decay curves are shown in Fig. 5. The distribution of residuals and chi-square values for glass and the SiFs system are given both above and below the respective time resolved decay curves. We observed that tinopal decays single exponentially, with a decay time of 1.20 ns in between the glass–quartz sandwich system, which is similar to the literature [5] value. In the presence of SiFs, the tinopal fluorescence decay is more complex and is best described by a bi-exponential function with decay components 1.20 and 0.11 ns. The amplitudes of these decay components are ≈ 30% and ≈ 70% respectively. The longer decay component is thought to indicate the free space component of tinopal, while the short decay component indicates the close proximity of the tinopal to the SiFs, consistent with reports of other fluorophores near-to silver nano particles [4–6].

In order to further understand metal-enhanced tinopal fluorescence, we have also measured the photostability of tinopal in aqueous solutions from between quartz and also from a quartz–SiFs sandwich. These samples were exposed to a 405 nm laser line for about 300 s and the steady state fluorescence measured with time, are shown in Fig. 6. The photostability of the tinopal increases on SiFs as compared to the glass control i.e. more photons are observed

Table 1
Decay parameters of Tinopal on SiFs–quartz and Glass quartz sandwich.

Sample	τ_1 (ns)	α_1 %	τ_2 (ns)	α_2 %	$\langle \tau \rangle$	$\bar{\tau}$	χ^2
Glass–Quartz	1.19 ± 0.02	100	–	–	1.19	1.19	1.121
SiFs–Quartz	1.20 ± 0.05	30	0.11 ± 0.02	70	1.00	0.44	1.237

$\langle \tau \rangle$ is amplitude weighted decay time and $\bar{\tau}$ is mean decay time.

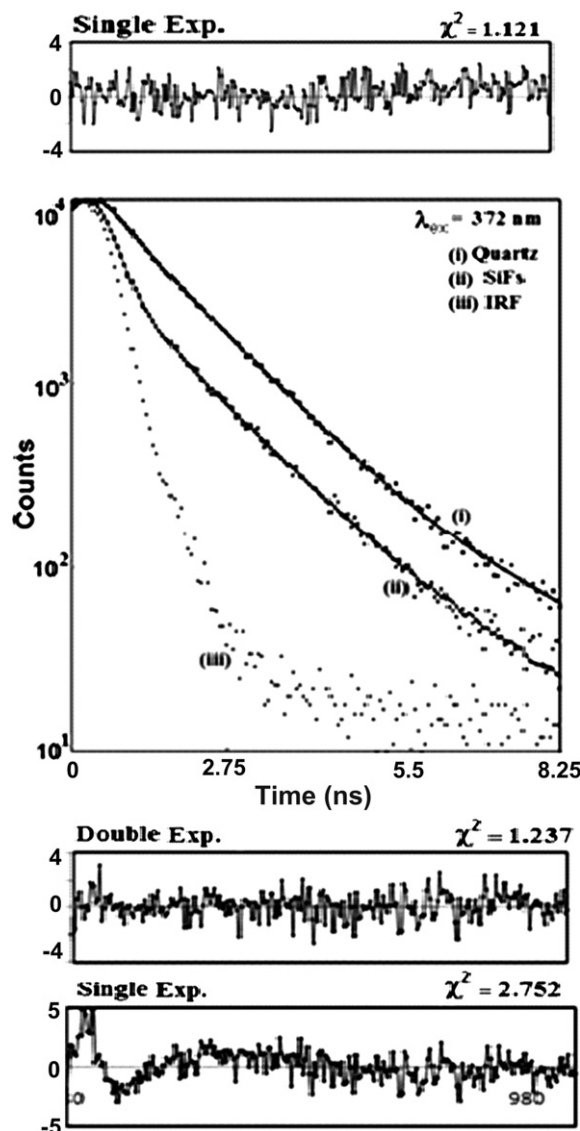


Fig. 5. Decay Profile of Tinopal on a Quartz slide and SiFs $\lambda_{exc} = 372$ nm. Residuals of the best fit functions for quartz slides and SiFs are given above and below respectively.

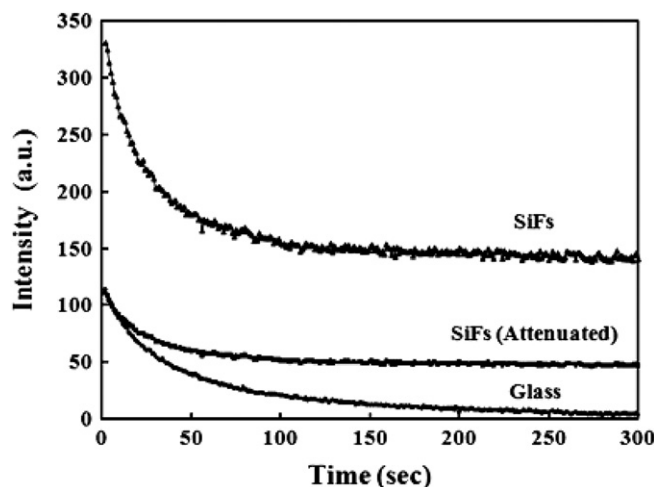


Fig. 6. Steady-state intensity vs. time (photostability) of Tinopal on a glass slide and on SiFs. To further demonstrate the benefit of SiFs, the laser power on SiFs was attenuated to give the same initial steady-state intensity as was observed on glass.

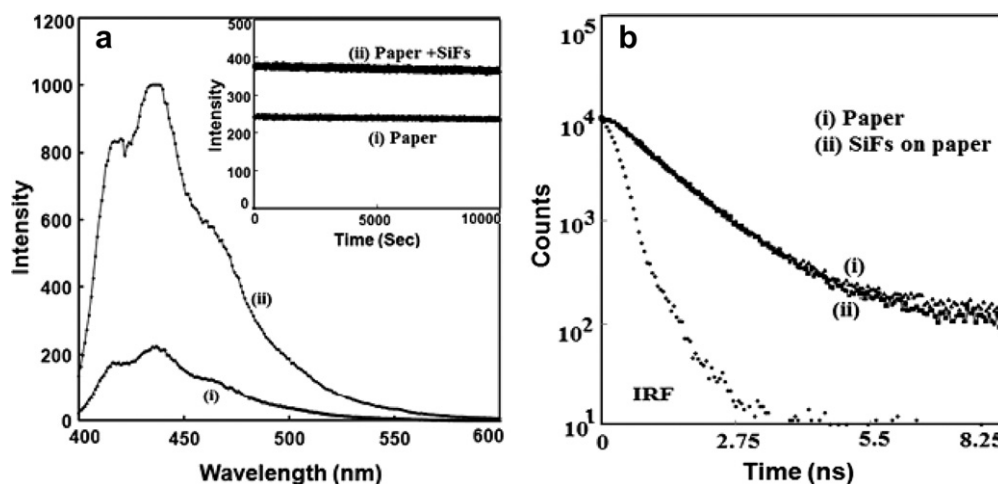


Fig. 7. (a) Fluorescence spectra and photostability (inset), (b) decay curves of tinopal on (i) paper and (ii) SiFs on paper.

per unit time. This finding is consistent with the reduced decaytime of tinopal near-to SiFs, Table 1, i.e. a reduced decay time and enhanced fluorescence photostability.

Given the use of optical brighteners in paper formulations, we have also deposited silver nano particles onto paper. The overlapped fluorescence spectra and decay curves of tinopal on cellulose filter paper (control) and on colloidal silver deposited cellulose filter paper are shown in Fig. 7(a) and (b) respectively. It is found that the fluorescence intensity is also enhanced about 4.5 fold due to the presence of the impregnated silver nano particles, but surprisingly no change in decay profile was observed. An additional decay time of 2.5 ns along with a 1.2 ns decay time component is observed where the 2.5 ns component is thought due to binding of some of the tinopal molecules to the cellulose fibers [11]. To understand this effect, photo bleaching experiments were also undertaken for both silver and the control paper. Tinopal was found to be highly photo-stable from both these papers and no notable effect of the silver nano particles was observed, consistent with our observation of no change in decay time.

The photo-physics of tinopal is shown to be drastically and favorably changed on SiFs deposited glass slides and also from papers as compared to uncoated slides and uncoated paper respectively. About ≈ 4.5 fold enhancement in far-field tinopal fluorescence is observed with near-field enhancement values about 50 fold greater, i.e. 225-fold as compared to a control sample containing no silver. Two photophysical processes are typically thought to underpin MEF. The first is an electric field effect in which molecules in close proximity (<10 nm) to silver nanoparticles are exposed to the increased electric fields in between and around the plasmonic nanoparticles, resulting in significant increases in their effective absorption cross section. This lends itself to a subsequent increase in the excitation and eventually in the fluorescence emission from the tinopal, while the decay time remains unchanged.

In the second process, coupling of the excited states of fluorophores to surface plasmons occurs where the excited-state energies of fluorophores are partially transferred to surface plasmons (induced mirror dipoles). Two distinct observations can therefore be made for fluorescent species in close proximity to plasmonic nanoparticles: (1) an increase in the fluorescence emission from the metal-fluorophore *unified* system with the spectral properties of the fluorophores maintained, and (2) a reduction in the fluorescence lifetime, giving rise to improvements in the photostability of the fluorophores. For tinopal, we subsequently propose that there are two populations of adsorbed

molecules on the SiFs coated glass slide: one population is composed of more isolated molecules far from the SiFs, the photophysical properties of these similar to tinopal in the far-field condition. In the near field i.e. near to silver, an enhanced absorption and coupling to plasmons facilitates metal enhanced tinopal fluorescence as well as an enhanced photostability.

MEF from paper substrates can potentially be developed for high-throughput surface analysis, such as surface based immunoassays given the low cost of paper and other cellulose based products. The MEF technology could also be used as an anti-counterfeiting measure from paper, whereby dyes/fluorophore's proximity to silver, affords for enhanced luminescence signatures, reduced lifetimes, directional luminescence and enhanced photostabilities. It is also highly unlikely that these fluorophore-metal system properties can be counterfeited by generic printing/copying press methodologies. Given the significant advances in ink jet printing technology [22], it is highly likely that silver nanoparticles can be printed onto paper substrates [23]. Patterned paper could then find numerous applications in both anti-counterfeiting technologies and surface assay arrays [24]. Our findings are helpful in the development of enhanced optical brighteners for potential applications on both textiles and papers. Work is currently underway in our laboratory in this regard.

4. Conclusion

In this paper, we have reported metal-enhanced absorption, emission and photostability of Tinopal in close proximity to SiFs and silver adsorbed cellulose paper as compared to an identical control sample containing no silver. Our findings enhanced optical brighteners These findings are helpful in the development of enhanced luminescence and prolonged photostability of optical brightener for potential applications on textiles and papers.

Acknowledgment

The authors acknowledge the Institute of fluorescence, (IoF) and department of Chemistry and Biochemistry, UMBC, Baltimore, Maryland, USA, for salary support.

References

- [1] Geddes CD. Metal-enhanced fluorescence. USA: Wiley International; 2010. pp. 1–24, ISBN 978-0-470-22838-8.

- [2] Geddes CD. In: Geddes CD, Lakowicz JR, editors. Radiative decay engineering. Topics in fluorescence spectroscopy, vol. 8. New York: Springer; 2004.
- [3] Geddes CD, Lakowicz JR. Metal-enhanced fluorescence. *J Fluorescence* 2002;12:121–9.
- [4] Aslan K, Lakowicz JR, Szmajcinski H, Geddes CD. Metal-enhanced fluorescence solution-based sensing platform. *J Fluorescence* 2004;14:677–9.
- [5] Aslan K, Geddes CD. Directional surface plasmon coupled luminescence for analytical sensing applications: which metal, what wavelength, what observation angle. *Anal Chem* 2009;81:6913–22.
- [6] Zhang Y, Aslan K, Previte MJR, Geddes CD. Metal-enhanced fluorescence from paper substrates: modified spectral properties of dyes for potential high-throughput surface analysis and assays and as an anti-counterfeiting technology. *Dyes Pigments* 2008;77(3):545–9.
- [7] Aslan K, Geddes CD. Metal-enhanced chemiluminescence: advanced chemiluminescence concepts for the 21st century. *Chem Soc Rev* 2009;38:2556–64.
- [8] Yamaki SB, Barros SB, Garcia GMZ, Socoloski P, Oliveira ON, Atvars TDZ. Spectroscopic studies of the intermolecular interactions of congo red and tinopal CBS with modified cellulose fibers. *Langmuir* 2005;21:5414–20.
- [9] Iamazaki EI, Atvars TDZ. Role of surfactants in the sorption of the whitening agent tinopal CBS onto viscose fibers: a fluorescence spectroscopy study. *Langmuir* 2006;22:9866–73.
- [10] Iamazaki EI, Atvars TDZ. Sorption of a fluorescent whitening agent (Tinopal CBS) onto modified cellulose fibers in the presence of surfactants and salt. *Langmuir* 2007;23:12886–92.
- [11] Damant AP, Castle L. Determination of fluorescent whitening agents in paper and board packaging materials by capillary electrophoresis. *J Microcolumn Separat* 1999;11(4):259–62.
- [12] Shu WC, Ding WH. Determination of fluorescent whitening agents in laundry detergents and surface waters by solid-phase extraction and ion-pair high-performance liquid chromatography. *J Chromatogr A* 2005;1088:218–33.
- [13] Hartela PG, Hagedorn C, McDonaldb JL, Fishera JA, Salutad MA, Dickerson JW, et al. Exposing water samples to ultraviolet light improves fluorometry for detecting human fecal contamination. *Water Res* 2007;41:3629–32.
- [14] Green LK, Ansari MQ, Schwartz MR, Ro JY, Alpert LC. Non-specific fluorescent whitener stains in the rapid recognition of pulmonary dirofilariasis: a report of 20 cases. *Thorax* 1994;49:590–3.
- [15] Arakawa T, Kamimura M, Furuta Y, Miyazawa M, Kato M. Peroral infection of nuclear polyhedrosis virus budded particles in the host *Bombyx mori* L. enabled by an optical brightener, Tinopal UNPA-GX. *J Virol Method* 2000;88:145–52.
- [16] Goulson D, Derwent LC, Penagos DI, Williams T. Effects of optical brighteners included in biopesticide formulations on the growth of crops. *Agri Eco Environ* 2003;95:235–40.
- [17] Goulson D, Marti'nez AM, Hughes WOH, Williams T. Effects of optical brighteners used in biopesticide formulations on the behavior of pollinators. *Biol Contr* 2000;19:232–6.
- [18] Marti'nez AM, Goulson D, Chapman WJ, Caballero P, Cave DR, Williams T. Is it feasible to use optical brightener technology with a baculovirus bioinsecticide for resource-poor maize farmers in mesoamerica? *Biol Control* 2000;17:174–81.
- [19] Morales L, Moscardi F, Sosa-Go'mez RD, Paro EF, Soldorio LR. Fluorescent brighteners improve *Anticarsia gemmatalis* (Lepidoptera: Noctuidae) nucleopolyhedrovirus (AgMNPV) activity on AgMNPV susceptible and resistant strains of the insect. *Biol Control* 2001;20:247–53.
- [20] Barbera JAS, Parkinb CS. Fluorescent tracer technique for measuring the quantity of pesticide deposited to soil following spray applications. *Crop Protect* 2003;22:15–8.
- [21] Sarrazin P, Beneventi D, Chaussy D, Vurth L, Stephan O. Adsorption of cationic photo luminescent nano particles on softwood cellulose fibers: effects of particles stabilization and fibers' beating. *Collo Surf* 2009;334:80–3.
- [22] Magdassi S, Bassa A, Vinetsky Y, Kamyshny A. Silver nanoparticles as pigments for water-based ink-jet inks. *Chem Mater* 2003;15(11):2208–17.
- [23] Sametband M, Shweky I, Banin U, Mandler D, Almog J. Application of nanoparticles for the enhancement of latent fingerprints. *Chem Commun* 2007;11:1142–4.
- [24] Hardwick B, Jackson W, Wilson G, Mau AWH. Advanced materials for bank-note applications. *Advan Mater* 2001;13(12–13):980–4.